Realization of an atomically flat $BaSnO_3(001)$ substrate with SnO_2 termination

Woong-Jhae Lee,[1] Hwangho Lee,[2] Kyung-Tae Ko,[2] Jeonghun Kang,[1] Hyung Joon Kim,[1] Takhee Lee,[3] Jae-Hoon Park,[2,4] and Kee Hoon Kim[1,3,a)]
[1]*Center for Novel States of Complex Materials Research, Department of Physics and Astronomy, Seoul National University, Seoul 08826, South Korea*
[2]*Max Planck POSTECH Center for Complex Phase Materials and Department of Physics, Pohang University of Science and Technology, Pohang 37673, South Korea*
[3]*Department of Physics and Astronomy, Institute of Applied Physics, Seoul National University, Seoul 08826, South Korea*
[4]*Division of Advanced Material Science, Pohang University of Science and Technology, Pohang 37673, South Korea*

(Received 22 July 2017; accepted 14 November 2017; published online 6 December 2017)

Atomically flat terraces terminated by mostly single layer SnO_2 are realized on the surface of a $BaSnO_3(001)$ substrate with a lateral dimension of about $3 \times 3\,mm^2$ by deionized water leaching and thermal annealing. Surface topography studies reveal that by controlling the annealing time and temperature, the topmost surface evolves from having chemically mixed termination to atomically flat terraces with a step height of one unit cell. The step bunching and kinked steps also depend sensitively on the out-of-plane and in-plane miscut angles. X-ray photoemission spectroscopy near the $Ba3d_{5/2}$ and $Sn3d_{5/2}$ states with variation in the electron emission angle confirmed that the topmost atomic layer of the $BaSnO_{3-\delta}(001)$ surface mostly consisted of SnO_2 rather than BaO. The present findings will facilitate the preparation of atomically flat $BaSnO_3(001)$ substrates, which will be useful in the studies of exploring possible two-dimensional electron gases at the interface between $BaSnO_3(001)$ and other oxides. *Published by AIP Publishing.*
https://doi.org/10.1063/1.4997238

Barium stannate ($BaSnO_3$) is an attractive, wide bandgap (~3.1 eV) semiconductor that has drawn increasing recent attention in the field of oxide electronics. Similar to the archetypal oxide $SrTiO_3$, it has a cubic perovskite structure with a lattice constant of ~4.116 Å, consisting of alternating stacks of BaO and SnO_2 layers [as shown in Figs. 1(a) and 1(b)]. Upon doping with lanthanum to generate an electron doping level of $\sim 1 \times 10^{20}\,cm^{-3}$, $BaSnO_3$ has been shown to exhibit an electron mobility of $320\,cm^2\,V^{-1}s^{-1}$ at room temperature,[1,2] which corresponds to one of the highest values realized among oxides at this temperature.[3] Such a high mobility of $BaSnO_3$ is understood as arising both from a large dispersion of the conduction band with a low electron effective mass of ~0.2–0.4m_0 (Refs. 4–6) and from the reduced ionized-impurity scattering related to its high dielectric constant of ~20.[7,8] Moreover, $BaSnO_3$ exhibits high optical transparency and good thermal stability, making it attractive for applications related to transparent oxide electronics.[1–3]

Currently, there is active worldwide research being undertaken to increase electron mobility in doped-$BaSnO_3$ films through various methods, e.g., defect minimization.[9–11] Forming oxide based two-dimensional electron gases (2DEGs) via heterostructure engineering could be yet another promising route to realize high electron mobility at ambient temperature. Several theoretical predictions have recently proposed that 2DEGs could be realized in a $BaSnO_3$-based heterostructure if $BaSnO_3$ as the channel material forms a sharp interface with other transparent oxides.[12–14] In contrast to those theoretical predictions, experimental activity is still in a nascent stage.[15,16] To realize 2DEGs in a $BaSnO_3$-based heterostructure, it is essential to have a $BaSnO_3(001)$ substrate with an atomically flat surface and terminated by a single oxide layer. However, the surfaces of most $ABO_3(001)$ substrates obtained by cleaving, cutting, or polishing result in mixed domains with AO- and BO_2-termination. It is known that chemically mixed termination can be converted into an atomically flat and single oxide terminating surface with step-terrace structures by performing effective solution etching and/or thermal annealing, which is well established in, e.g., $SrTiO_3$.[17–19]

In this letter, we report on the realization of atomically flat, mostly single-oxide terminated surfaces of $BaSnO_3(001)$ substrates by applying the sequential processing steps: careful polishing of the substrate with minimal miscut angles, quick deionized water leaching, and effective thermal annealing. The effects of substrate miscut angles on the step bunching and kinked step behaviors are also investigated. From the Ba^{2+} and Sn^{4+} signals in the 3*d* core-level spectra in combination with atomic force microscopy (AFM), we demonstrate that the topmost surfaces of the $BaSnO_3(001)$ substrates were almost exclusively composed of SnO_2-terminating terraces with a single unit step between neighboring terraces. The maximum lateral dimension of one terrace was as large as $2 \times 0.5\,\mu m^2$.

$BaSnO_{3-\delta}$ ($BaSnO_3$) single crystals were grown using polycrystalline $BaSnO_3$ as the seed and a mixture of CuO, Cu_2O, and $KClO_4$ powders as the flux, of which the molar ratio was adjusted to be $BaSnO_3$:CuO:Cu_2O:$KClO_4$ = 1:22.4:27.6:0(2).[9] The grown $BaSnO_3$ and $BaSnO_{3-\delta}$

a)Electronic mail: khkim@phya.snu.ac.kr

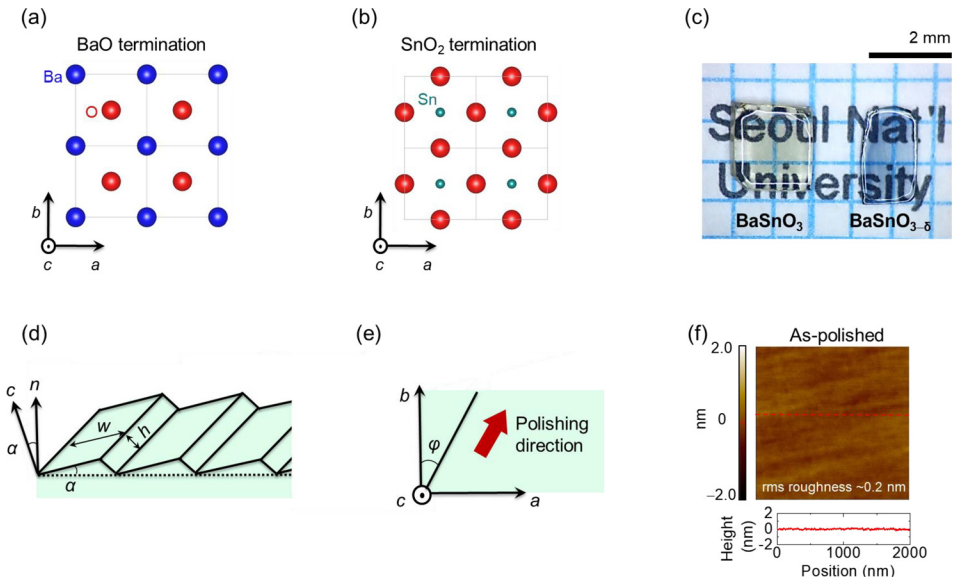

FIG. 1. The top views of (a) BaO and (b) SnO_2 surfaces of $2 \times 2 \times 2$ cells of cubic perovskite $BaSnO_3$. (c) Polished $BaSnO_3(001)$ and $BaSnO_{3-\delta}(001)$ single crystals grown by the CuO/Cu_2O flux method. (d) Schematic of a substrate with miscut angles. The out-of-plane miscut angle α is atan(H/W). L and W are the terrace width and step height, respectively. (e) Top view of a surface where the steps show an in-plane miscut angle φ with respect to the b axis of the cubic perovskite structure. (f) Surface morphology and height profile of the polished $BaSnO_3(001)$ substrate. The height profile is taken along the dotted solid line.

single crystals were chemically and mechanically polished to have an atomically flat surface. Before polishing, the *ab*-plane of the sample with a cube shape was attached to the flat surface of a polishing chuck, of which the surface normal axis could be slightly tilted by $\theta_{off} = \sim 0.05° – 1.0°$ during the polishing process. In this way, the terrace width could be controlled via the tilting angle as the width became roughly proportional to $1/\tan\theta_{off}$. Mechanical polishing was performed using polishing cloths and colloidal silica suspensions in a polishing machine (Allied High Tech Products). After each polish, the out-of-plane (in-plane) miscut angle was measured from the ω-scan (ϕ scan) of the (002) peaks using a high-resolution X-ray diffractometer (Empyrean^{TM}, PANalytical). The polished $BaSnO_3(001)$ and $BaSnO_{3-\delta}(001)$ surfaces were cleaned using microorganic soap, acetone, ethanol, and isopropanol. The cleaned substrates were agitated in deionized water for about 10 s. Thermal annealing was carried out in a resistive heating furnace using an alumina tube at various temperatures between 1000 and 1300 °C with a ramping rate of ~600 °C/h and for different durations of 2–100 min in 1 atm O_2 flow with a flow rate of 10 ml/min. At the end of the heating period, the substrate was furnace-cooled to room temperature at a rate of ~600 °C/h. The surface morphology was studied by atomic force microscopy (AFM) (NX10^{TM}, Park Systems) at room temperature, after the substrates were removed from the tube furnace. We confirmed that the morphology of the thermally annealed surface as probed by the AFM remained almost the same even after six months in dry air, indicating superior surface stability. In order to examine the surface termination, we performed angle-dependent X-ray photoemission spectroscopy (XPS) using Al-Kα (1486.7 eV). Before loading the samples into the ultra-high vacuum (UHV) chamber, the surfaces of the substrates were exposed to air during the transfer from the furnace and were not heated inside the chamber. All the photoemission spectra were measured at room temperature. To prevent charging effects in the XPS measurements, conducting $BaSnO_{3-\delta}(001)$ substrates with slight oxygen deficiency,[3] thus having electron doping, were prepared.

Figure 1(c) shows the transparent $BaSnO_3(001)$ and $BaSnO_{3-\delta}(001)$ substrates grown by the flux method. In contrast to the $BaSnO_{3-\delta}(001)$ substrate showing a metallic resistivity of 1 mΩ cm, the $BaSnO_3(001)$ substrate exhibited highly insulating behavior reaching a resistivity of $\sim 10^{12}$ mΩ·cm at room temperature.[9] The crystal miscut angles are known to be crucial parameters for producing terraced nanostructures on a surface.[20] To obtain a well-defined topography of terraces with parallel steps, we polished the sample surface by considering two miscut angles, i.e., the out-of-plane miscut angle $\alpha = \text{atan}(H/W)$ and the in-plane miscut angle φ, where H and W were the height and width of the terrace, respectively. Figures 1(d) and 1(e) display schematically the two miscut angles of α and φ. During the polishing procedure, α and φ were carefully controlled by tilting the single crystals to result in the variation of α from 0.05° to 1.0° and the variation of φ from 0° to 45°. After the etching and thermal treatment, we found that the change of α from 0.1° to 1.0° resulted in the variation of one terrace width from 230 to 23 nm. Moreover, between two terraces in close proximity with the same termination type, a step of one unit cell (u.c.) height, i.e., 4.116 Å, was formed.

The AFM study of the as-polished $BaSnO_3(001)$ substrate showed a root-mean-square (rms) roughness of ~0.2 nm [Fig. 1(f)]. Since the rms roughness of commercial $SrTiO_3(001)$ substrates is typically around 0.1 nm, the rms roughness of ~0.2 nm in the as-polished surface before chemical etching and heat treatment seems reasonable. Moreover, the polished $BaSnO_{3-\delta}(001)$ substrates showed a similar surface morphology with an rms roughness of ~0.2 nm (not shown here).

In general, the chemical control of the topmost surface termination can be realized by electronic reconstruction, changes in stoichiometry (i.e., atomic reconstruction), or a combination of both electronic and atomic reconstructions.[19] For this, one usually applies several processes such as acidic solution etching, thermal annealing, or both acidic solution etching and thermal annealing.[20] In our case, after cleaning the as-polished surface, the substrates were agitated in deionized water for 10 s to achieve weak surface etching. The substrates were subsequently annealed in the tube furnace. Figure 2 shows the AFM topography images, illustrating how the surface texture of the $BaSnO_3(001)$ substrates progressively transformed by thermal annealing. No change in

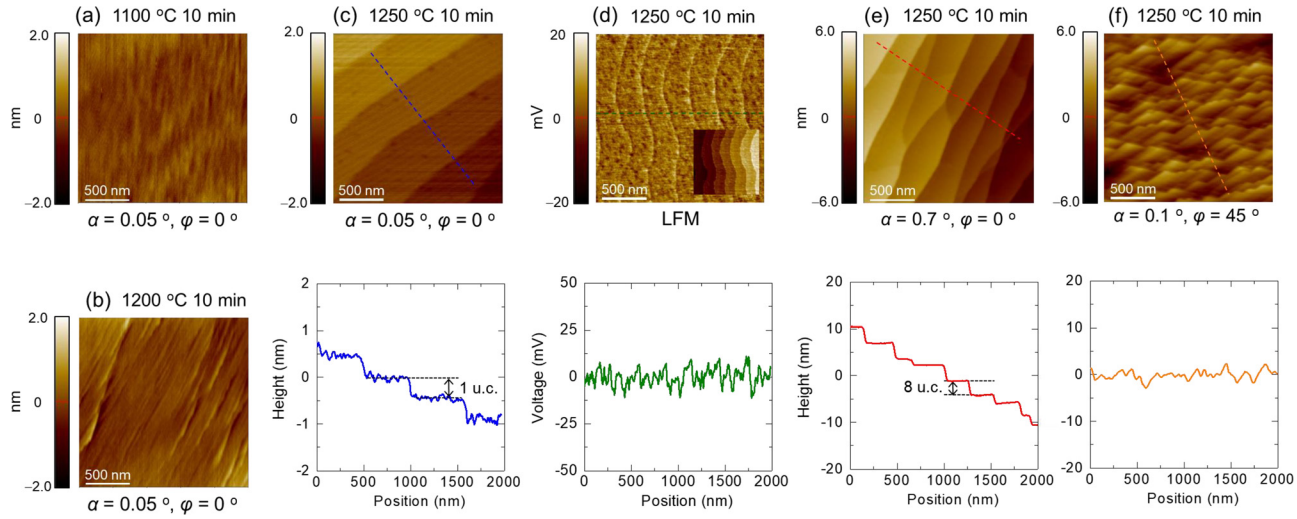

FIG. 2. AFM topographic images of $BaSnO_3(100)$ substrates after the process of etching in deionized water followed by thermal annealing at (a) 1100 °C, (b) 1200 °C, and (c) 1250 °C for 10 min in an O_2 atmosphere. In (a)–(c), the samples were pre-polished to have small out-of-plane ($\alpha = 0.05°$) and in-plane miscut angles ($\varphi = 0°$). (d) Lateral force microscopy (LFM) profile of the $BaSnO_3(001)$ substrate after deionized-water leaching followed by thermal annealing at 1250 °C for 10 min in an O_2 atmosphere. The inset shows the corresponding AFM topography. In the bottom panel of (d), the line profile of the LFM signal is also shown. Another AFM topographic images of $BaSnO_3(001)$ substrates obtained after polishing with (e) large $\alpha = 0.7°$ and (f) large $\varphi = 45°$ are shown, followed by thermal annealing at 1250 °C for 10 min in an O_2 atmosphere. In the bottom panels of (c), (e), and (f), the height-profile measured along the dotted line in each topographic image is also shown.

the surface morphology occurred in the thermal annealing process below 1100 °C as compared with the as-polished surface. Upon annealing at 1100 °C for 10 min in an O_2 flow atmosphere, however, a small corrugation started to appear [Fig. 2(a)]. This indicates that the thermal annealing at 1100 °C produced electronic and atomic reconstructions. At this stage, the topmost surface seemed to be still composed of mixed-chemical terminations, i.e., both SnO_2 and BaO terminations [as shown in Figs. 1(a) and 1(b)].

When the $BaSnO_3(001)$ substrate was annealed at 1200 °C for 10 min in O_2 flow, the surface showed the formation of partially aligned, stripe-like patterns, which might have developed further into step edges [Fig. 2(b)]. However, even by increasing the annealing time up to 1 h at 1200 °C, the surface did not exhibit any further noticeable morphological changes. Therefore, the annealing condition was adjusted to 1250 °C for 10 min under O_2 flow, which produced atomically flat and wide terrace regions, as seen in Fig. 2(c). The resultant mean-terrace-width was about 500 nm, and each step was one u.c. in height (~4.116 Å) with parallel steps. We found that this kind of wide terrace could be formed when the miscut angle α was adjusted to be less than 0.1° before polishing. α less than 0.1° was also confirmed by the X-ray ω-scan. As a result, the rms roughness within a terrace did not exceed 1 Å. The line profile measured along the dotted line, shown in the bottom panel of Fig. 2(c), exhibits only single unit cell steps of $BaSnO_3$ within the AFM resolution, which is ~0.5 Å along the z-axis. Moreover, from lateral force microscopy on the equally treated $BaSnO_3(001)$ substrates, we observed that the terrace surface showed a uniform frictional response [Fig. 2(d)], which again supports that the substrate was terminated by a single layer. This result was reproduced for many of the equally treated $BaSnO_3(001)$ substrates and for the $BaSnO_{3-\delta}(001)$ substrates. All these observations consistently support that the topmost surface layer is terminated with one kind of chemical layer such as BaO or SnO_2 [Figs. 1(a) and 1(b)].

To check how the surface morphology varied with increasing α, the $BaSnO_3(001)$ substrates having relatively large values of α were investigated after the same heat treatment, i.e., 1250 °C for 10 min under O_2 flow. Figure 2(e) shows an AFM image of the $BaSnO_3(001)$ substrate with $\alpha = 0.7°$ and $\varphi = 0°$; it displays a characteristic feature that the terrace width growth is delimited by having crossed facets between neighboring step edges. The average terrace width was ~250 nm, and the height profiles showed step edges with a height of ~4–8 u.c., which agrees with the miscut angle extracted by the X-ray ω-scan. This step-bunching formation is consistent with that observed in $SrTiO_3(001)$[21] and Si(113)[22] substrates with α values close to 0.2° and 1.7°, respectively. Furthermore, in order to check the effect of φ, $BaSnO_3(001)$ substrates having large φ were also investigated. Figure 2(f) presents the surface morphology of a $BaSnO_3(001)$ substrate with $\alpha = 0.1°$ and $\varphi = 45°$, in which significant step-edge meandering and sharp triangular shape domains were found. It is known that the presence of such triangular-shaped domains could be associated with a large value of φ.[20] A similar morphological feature has also been reported in $SrTiO_3(001)$ substrates prepared with high values of φ of ~6° and 35°.[21,23]

To determine the nature of the surface termination layer, XPS was used to characterize the $BaSnO_{3-\delta}(001)$ surface, which had a large terrace width of ~500 nm and step edges with a height of one u.c., as shown in Fig. 2(c). In particular, XPS measurements were performed at various photoemission angles θ with respect to the surface normal [Fig. 3(a)]. When θ is systematically increased from 0° to 70°, it is expected that the surface contribution to the spectra will increase considerably.[24,25] In other words, at high θ values, the effective electron escape depth described as $\lambda_{eff} = \lambda\cos\theta$ (λ: mean free path of escaping electrons) should decrease, which should lead to an increase in the relative photoelectron intensities of Sn3d if the terminated layer consists of SnO_2.

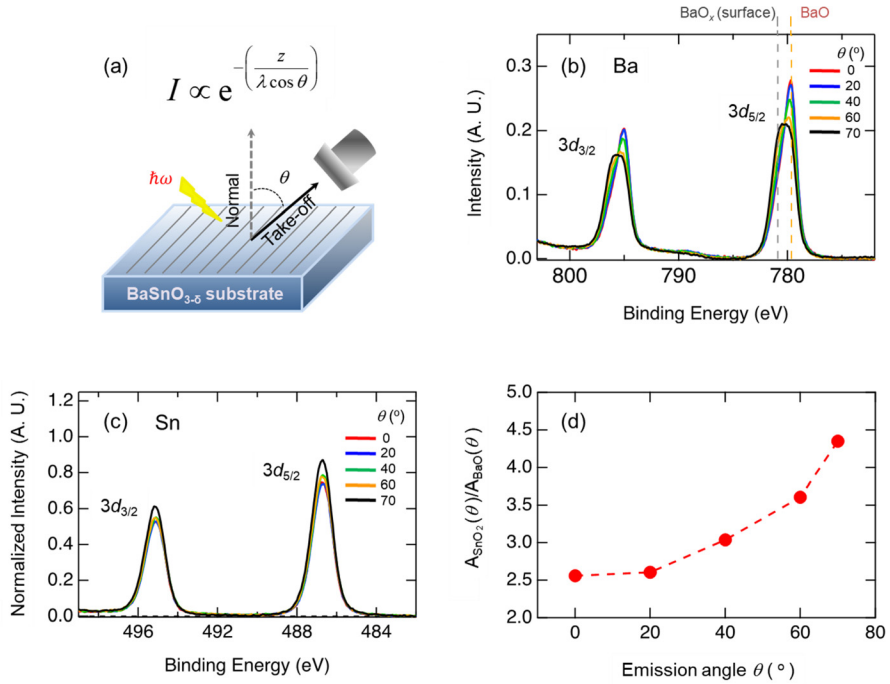

FIG. 3. (a) A schematic plot illustrating angle-dependent X-ray photoemission spectroscopy. Spectral intensity I is proportional to $\exp[-z/(\lambda\cos\theta)]$, where z, λ, and θ correspond to the depth of atoms, the mean free path of escaping electrons, and the emission angle, respectively. Photoemission spectra of (b) Ba3d and (c) Sn3d states of $BaSnO_{3-\delta}(001)$ substrates with various θ are shown. (d) The area ratio of the $3d_{5/2}$ states of SnO_2 and BaO at each θ $[A_{SnO_2}(\theta)/A_{BaO}(\theta)]$.

Therefore, one can identify the termination layer by comparing the photoelectron intensities of each cation at different θ.

In Fig. 3(b), the spectra of Ba3d core-levels measured at various θ are displayed. First, the spectra of Ba3d normalized with the total area after subtracting backgrounds show the change in the spectral weight. The spectra exhibit $d_{5/2}$ and $d_{3/2}$ white lines because of the large spin-orbit splitting of a core hole. The spectral intensity is systematically reduced at higher θ, as expected. The main peak centered at a low binding energy of 779.65 eV in the $3d_{5/2}$ white lines is well known to be from bulk BaO.[26] Additional small intensity centered at a slightly high binding peak at 780.9 eV is noticeable and can be attributed to barium oxide in the topmost surface, which is usually under-coordinated compared to bulk BaO. Thus, it is denoted here as BaO_x. According to several studies on the core level spectra of surface Ba, BaO, and under-coordinated BaO_x,[27–29] the appearance of core level spectra at a slightly higher binding energy can be attributed to topmost BaO_x. As can be seen in Fig. 3(b), with an increase in θ, the intensity of the bulk BaO peak (779.65 eV) decreased systematically, whereas that of the surface BaO_x peak (780.9 eV), albeit small, remained almost constant. Since the spectrum using the high take-off angle is more surface-sensitive, this information suggests that a small fraction of residual BaO_x still remained on the topmost surface. In other words, although the 2×2 μm^2 surface morphology in the AFM image does not show any evidence of other residual particles except single-layer termination, there appears to exist a small amount of BaO_x in the surface region. The residual BaO_x in the topmost surface may have formed potentially because of Ba segregation from the bulk to the surface and oxidation during the annealing process in O_2. This BaO_x on the surface should be reduced in future work by optimizing the etching and annealing conditions.

To get more information on the dominant termination layer, the core level spectra of Sn3d were also measured at each θ. Figure 3(c) displays the core level spectra of Sn3d after subtracting backgrounds, which were well fitted by a pair of Voigt peaks where the Gaussian and Lorentzian broadening was fixed for each spectrum. A similar expression can also be used to describe the BaO spectra. The binding energy E_b for Sn3$d_{5/2}$ was 486.66 eV. To emphasize the relative intensity change depending on θ, the spectra were normalized with the spectral area of BaO (A_{BaO}), which was indeed the area of the Lorentzian peak located at $E_b = 779.65$ eV. As can be seen in Fig. 3(c), with an increase in θ, the intensity of the Sn3d spectra monotonically increased without any change in the spectral line shape.

To quantify the increase in the relative intensity, the ratio $[A_{SnO_2}(\theta)/A_{BaO}(\theta)]$ between the integrated areas of SnO_2 $A_{SnO_2}(\theta)$ and that of bulk BaO $A_{BaO}(\theta)$ was calculated at each θ in the case of the $3d_{5/2}$ states, as displayed in Fig. 3(d). It is clearly seen that the ratio of $A_{SnO_2}(\theta)/A_{BaO}(\theta)$ increased significantly at higher θ values, i.e., in the more surface-sensitive regime. Since the mean free path of escaping electrons, of which the kinetic energy is 700 eV (Ba3d) or 1000 eV (Sn3d), is ~10 Å, the intensity of the top layer atoms increased exponentially. Therefore, it is concluded that the measured spectra verify that the termination surface layer mostly consisted of SnO_2 rather than BaO. A similar analysis of angle-dependent XPS measurements has been reported for ZnO(0001) and $SrTiO_3(001)$ substrates.[24,30] Our work, thus, clearly shows that the atomically flat surfaces in both the grown $BaSnO_3(001)$ and $BaSnO_{3-\delta}(001)$ substrates were terminated mostly with SnO_2 layers with some small residual BaO_x in the surface region. Therefore, these substrates could become a useful platform for developing $BaSnO_3$-based heterostructures in combination with other wide bandgap oxides and for investigating the possible realization of 2DEGs, as predicted by recent theoretical works.

In conclusion, we have realized atomically flat surfaces of $BaSnO_3(001)$ and $BaSnO_{3-\delta}(001)$ substrates with a lateral size of $\sim 3 \times 3$ mm^2 and with 500-nm-wide terraces and step-edges with a height of one u.c. using deionized water

leaching followed by thermal annealing. By utilizing angle-dependent core-level photoelectron spectroscopy to estimate the area ratio of the $3d_{5/2}$ states of SnO_2 and BaO at each θ, we concluded that the termination of the $BaSnO_{3-\delta}(001)$ substrates mostly consisted of SnO_2. These experimental findings will be particularly useful in the study of exploring possible 2DEGs with high mobility at the interfaces between $BaSnO_3(001)$ and other band insulators.

This work was financially supported by the National Creative Research Initiative (2010-0018300) and the Korea-Taiwan Cooperation Program (0409-20150111) through the NRF of Korea and the Korea Institute of Energy Technology Evaluation and Planning funded by the Ministry of Trade, Industry, and Energy of Korea (20173010012940). T. Lee acknowledges the financial support of the National Creative Research Laboratory Program (Grant No. 2012026372) of Korea. H. Lee, K.-T. Ko, and J.-H. Park acknowledges the support of Study for Nano Scale Optomaterials and Complex Phase Materials (2016K1A4A4A01922028) through NRF of Korea.

[1]H. J. Kim, U. Kim, H. M. Kim, T. H. Kim, H. S. Mun, B.-G. Jeon, K. T. Hong, W.-J. Lee, C. Ju, K. H. Kim, and K. Char, Appl. Phys. Express **5**(6), 061102 (2012).
[2]H. J. Kim, U. Kim, T. H. Kim, J. Kim, H. M. Kim, B.-G. Jeon, W.-J. Lee, H. S. Mun, K. T. Hong, J. Yu, K. Char, and K. H. Kim, Phys. Rev. B **86**(16), 165205 (2012).
[3]W.-J. Lee, H. J. Kim, J. Kang, D. H. Jang, T. H. Kim, J. H. Lee, and K. H. Kim, Annu. Rev. Mater. Res. **47**(1), 391–423 (2017).
[4]D. Seo, K. Yu, Y. J. Chang, E. Sohn, K. H. Kim, and E. J. Choi, Appl. Phys. Lett. **104**(2), 022102 (2014).
[5]U. Kim, C. Park, T. Ha, R. Kim, H. S. Mun, H. M. Kim, H. J. Kim, T. H. Kim, N. Kim, J. Yu, K. H. Kim, J. H. Kim, and K. Char, APL Mater. **2**(5), 056107 (2014).
[6]H.-R. Liu, J.-H. Yang, H. J. Xiang, X. G. Gong, and S.-H. Wei, Appl. Phys. Lett. **102**(11), 112109 (2013).
[7]H. J. Kim, J. Kim, T. H. Kim, W.-J. Lee, B.-G. Jeon, J.-Y. Park, W. S. Choi, D. W. Jeong, S. H. Lee, J. Yu, T. W. Noh, and K. H. Kim, Phys. Rev. B **88**(12), 125204 (2013).
[8]W.-J. Lee, H. J. Kim, E. Sohn, H. M. Kim, T. H. Kim, K. Char, J. H. Kim, and K. H. Kim, Phys. Status Solidi A **212**(7), 1487–1493 (2015).
[9]W.-J. Lee, H. J. Kim, E. Sohn, T. H. Kim, J.-Y. Park, W. Park, H. Jeong, T. Lee, J. H. Kim, K.-Y. Choi, and K. H. Kim, Appl. Phys. Lett. **108**(8), 082105 (2016).
[10]S. Raghavan, T. Schumann, H. Kim, J. Y. Zhang, T. A. Cain, and S. Stemmer, APL Mater. **4**(1), 016106 (2016).
[11]Z. Lebens-Higgins, D. O. Scanlon, H. Paik, S. Sallis, Y. Nie, M. Uchida, N. F. Quackenbush, M. J. Wahila, G. E. Sterbinsky, D. A. Arena, J. C. Woicik, D. G. Schlom, and L. F. Piper, Phys. Rev. Lett. **116**(2), 027602 (2016).
[12]L. Bjaalie, B. Himmetoglu, L. Weston, A. Janotti, and G. C. Van de Walle, New J. Phys. **16**(2), 025005 (2014).
[13]X. Fan, W. Zheng, X. Chen, and D. J. Singh, PLoS One **9**(3), e91423 (2014).
[14]K. Krishnaswamy, L. Bjaalie, B. Himmetoglu, A. Janotti, L. Gordon, and C. G. Van de Walle, Appl. Phys. Lett. **108**(8), 083501 (2016).
[15]S. A. Chambers, T. C. Kaspar, A. Prakash, G. Haugstad, and B. Jalan, Appl. Phys. Lett. **108**(15), 152104 (2016).
[16]U. Kim, C. Park, Y. M. Kim, J. Shin, and K. Char, APL Mater. **4**(7), 071102 (2016).
[17]M. Kawasaki, K. Takahashi, T. Maeda, R. Tsuchiya, M. Shinohara, O. Ishiyama, T. Yonezawa, M. Yoshimoto, and H. Koinuma, Science **266**(5190), 1540–1542 (1994).
[18]G. Koster, B. L. Kropman, G. J. H. M. Rijnders, D. H. A. Blank, and H. Rogalla, Appl. Phys. Lett. **73**(20), 2920–2922 (1998).
[19]A. Biswas, C.-H. Yang, R. Ramesh, and Y. H. Jeong, Prog. Surf. Sci. **92**(2), 117–141 (2017).
[20]F. Sanchez, C. Ocal, and J. Fontcuberta, Chem. Soc. Rev. **43**(7), 2272–2285 (2014).
[21]R. Bachelet, F. Valle, I. C. Infante, F. Sánchez, and J. Fontcuberta, Appl. Phys. Lett. **91**(25), 251904 (2007).
[22]K. Sudoh and H. Iwasaki, Phys. Rev. Lett. **87**(21), 216103 (2001).
[23]G.-B. Cho, M. Yamamoto, and Y. Endo, Thin Solid Films **464–465**, 80–84 (2004).
[24]L. Zhang, D. Wett, R. Szargan, and T. Chassé, Surf. Interface Anal. **36**(11), 1479–1483 (2004).
[25]M. Sing, G. Berner, K. Goss, A. Muller, A. Ruff, A. Wetscherek, S. Thiel, J. Mannhart, S. A. Pauli, C. W. Schneider, P. R. Willmott, M. Gorgoi, F. Schafers, and R. Claessen, Phys. Rev. Lett. **102**(17), 176805 (2009).
[26]H. Van Doveren and J. Verhoeven, J. Electron. Spectrosc. Relat. Phenom. **21**(3), 265–273 (1980).
[27]D. M. Hill, H. M. Meyer III, and J. H. Weaver, Surf. Sci. **225**(1), 63–71 (1990).
[28]L. T. Hudson, R. L. Kurtz, S. W. Robey, D. Temple, and R. L. Stockbauer, Phys. Rev. B **47**(16), 10832–10838 (1993).
[29]P. Van der Heide, Surf. Sci. **490**(3), L619–L626 (2001).
[30]C. Baeumer, C. Xu, F. Gunkel, N. Raab, R. A. Heinen, A. Koehl, and R. Dittmann, Sci. Rep. **5**, 11829 (2015).